Orientation relationships of carlsbergite in schreibersite and kamacite in the north Chile iron meteorite

G. Nolze[1],*, G. Wagner[2], R. Saliwan Neumann[1], R. Skála[3] and V. Geist[2]

[1] Federal Institute for Materials Research and Testing, Unter den Eichen 87, 12205 Berlin, Germany
[2] Institute for Mineralogy, Crystallography and Materials Science, University of Leipzig, Scharnhorststrasse 20, 04275 Leipzig, Germany
[3] Institute of Geology, Academy of Sciences of the Czech Republic, Rozvojová 135, CZ-16502 Prague, Czech Republic

ABSTRACT

The crystallographic orientation of carlsbergite (CrN) in the north Chile meteorite (hexahedrite) was investigated using electron backscatter diffraction and transmission electron microscopy. These studies examined the CrN crystals in the rhabdites (idiomorphic schreibersite) and in kamacite. It was found that the CrN crystals embedded in rhabdite show a number of different orientation relationships with the host crystals. These orientations can be explained based on the lattice dimensions of both coexisting crystalline materials. It was also found that both carlsbergite and kamacite are characterized by a high dislocation density ($\geqslant 10^9$ cm^{-2}) while rhabdite is free of dislocations. It is supposed that in spite of the deformed metallic matrix, a general connection between the orientation relation of all the phases involved exists.

Keywords: EBSD, phosphides, carlsbergite, orientation relationship, iron meteorites.

Introduction

Kamacite and taenite represent the major phases contained in iron meteorites; other compounds such as carbides, nitrides, phosphides, chromites, sulfides, etc., are in subordinate amounts. It is assumed that the minor phases in iron meteorites are formed at different temperatures during the cooling in its parent body. Since the cooling rates are extremely slow (a few degrees per million years) and the precipitation of the minor phases is obviously a long process, one can also expect that distinct orientation relationships between the well crystallized matrix and all phases, or between the phases themselves have developed. In order to investigate local orientations, the EBSD (electron backscattered diffraction) technique has been established as powerful tool in scanning electron microscopy (SEM). Subsequently, over the last 5 years the orientation relationships between some of these phases have been investigated by this technique (Sevillano *et al.*, 2000; Schwarzer and Sukkau, 2003; Nolze and Geist, 2004; Nolze *et al.*, 2005; He *et al.*, 2006).

The north Chile iron meteorites (hexahedrites) are characterized by large single crystals of kamacite with a Ni content of <6%. The microstructure reflects a large amount of irregularly distributed tetragonal rhabdite crystals, which are small idiomorphic schreibersite crystals − (Fe,Ni)$_3$P − forming prismatic rods along [001] with {110} habit planes, cf. Bøggild (1927). The rod diameter is on the scale of 5−25 μm (Buchwald, 1975; Grady, 2000). The crystal structure of a meteoritic (Fe$_{1−x}$Ni$_x$)$_3$P was determined in 1970 by Doenitz (space-group type: $I\bar{4}$, a = 9.040 Å and c = 4.462 Å), but the lattice parameters vary distinctly with the Fe:Ni ratio of the phosphides (Fe/Ni $\approx$ 0.55−5.65) (Skála and Drábek, 2000; Skála and Císařová, 2005).

The orientation relationship between the kamacite matrix (subscript K) and the rhabdite rods (subscript R) was first described by Bøggild

* E-mail: gert.nolze@bam.de

(1927) investigating the hexahedrite Coahuila by light microscopy:

$$\{001\}_R \parallel \{001\}_K \text{ and } 110_R \parallel 210_K \qquad (1)$$

This was later confirmed for different iron meteorites using various techniques, e.g. Hennig *et al.* (1999). In the analysed piece of a north Chile iron, xenomorphic schreibersite grains have only been detected occasionally. In contrast to the rhabdite, they seem to show no special alignment to the surrounding kamacite orientation.

During the investigation of rhabdite, extracted from the north Chile iron for synchrotron experiments (Moretzki *et al.*, 2005), well shaped inclusions have been discovered. A closer view showed that these precipitates appear not only in the rhabdites but also in the metallic matrix (Figs 1, 2 and 4), cf. Buchwald (1975). The precipitates were identified as carlsbergite (CrN).

In iron meteorites, the carlsbergite mineral was first discovered in the Cape York and Charcas iron by Buchwald and Scott (1971). There, CrN appeared as minute laths in the kamacite, typically 30 µm × 5 µm × 2 µm in size. Moreover, it has been described as irregular 3−10 µm grains along some grain boundaries (Buchwald, 1975). The author also pointed out that carlsbergite is often associated with rhabdite. In comparison to rhabdite, carlsbergite is a relatively rare meteoritic mineral. The lattice parameter of the CrN (halite structure type, $Fm\bar{3}m$) is given by $a = 4.148(1)$ Å (Buchwald, 1975; Nasreddine *et al.*, 1977). To date, there

have been no known natural terrestrial occurrences of this mineral. Hitherto, carlsbergite has been identified in iron meteorites of the groups IAB, IIAB, IIIAB and IVA (cf. also Zipfel *et al.*, 1995). Axon *et al.* (1981) reported carlsbergite as an "unusual feathery feature penetrating into massive troilite of the Sikhote Alin iron" (IIAB).

The crystal structures of both CrN and $(Fe,Ni)_3P$ are composed of transition metal atoms and non-metal atoms of periodic group V. Both compounds are understood as the so-called 'interstitial solid solutions'. The metal-non metal atoms are combined by covalent bonds. Mutual interactions among the non-metals are weak in contrast to the bonding between metal atoms. This behaviour means that $(Fe,Ni)_3P$ and CrN are chemically related compounds, independent of their different crystal structures and lattice parameters.

The main goal of this paper is the determination of the orientation relationship of CrN crystals with respect to other phases in the north Chile iron. Because of their tiny size neither a crystallographic description nor the orientation relationship between CrN and the respective host crystal has been reported previously.

Experimental

Material

The north Chile shower consists of eight individual iron meteorites, identical in structure and composition. Although they have been found
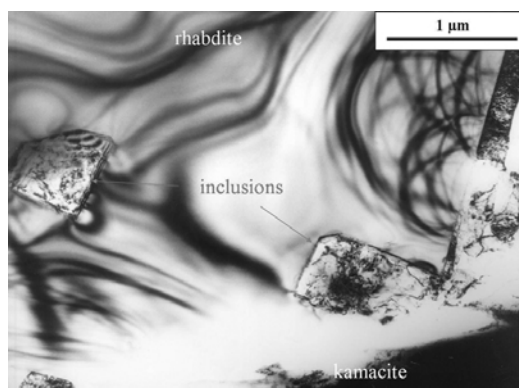

FIG. 1. TEM bright-field image of CrN inclusions inside a larger, dislocation-free rhabdite crystal. A complex dislocation structure is visible in CrN. The composition of the rhabdite was determined to be 43 at.% Fe, 32 at.% Ni and 25 at.% P.
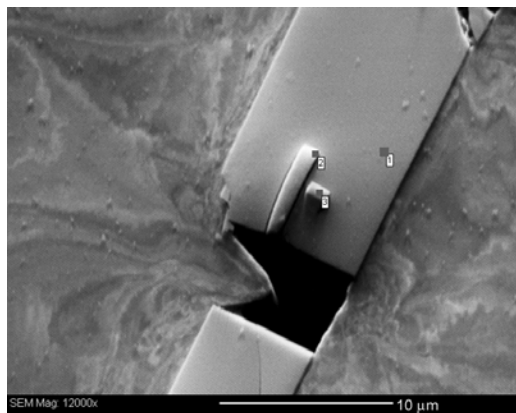

FIG. 2. BSE image of a cracked rhabdite crystal containing two carlsbergites. At the marked positions (1, 2, 3), EBSD patterns have been recorded. The contrast change in kamacite displays orientation variations caused by plastic flow.

in the same area, the exact localities are unclear (Grady, 2000). The investigated piece was purchased from the mineral company F. Krantz in Bonn, Germany, and is believed to represent the Tocopilla mass. It is a triangular plate, ~2 mm thick and 20 mm in its largest dimension. The sample was prepared as for a typical metallographic investigation: ground with abrasive paper (up to 1200) and subsequently polished with diamond paste (down to 0.25 μm). For the EBSD measurements a final polishing by colloidal silica has been applied in order to remove all residual surface irregularities. This is required because the quality of electron diffraction patterns is extremely sensitive to even slight surface damages caused by the mechanical grinding and polishing.

TEM

For the characterization of small sample volumes, transmission electron microscopy (TEM) is the preferred technique (e.g. Fultz and Howe, 2005). For all investigations, a Philips CM 200 has been used. In order to produce electron-transparent sections with a thickness of ~10−40 nm, Ar^+ ion milling was applied (4 kV, 0.5 mA, incidence angle 13º). The chemical composition of phases was determined with an attached EDS detector (Si(Li) detector with a SUTW (super ultra thin window)). The lateral resolution in nano-probe mode used for chemical analysis is commonly assumed to be ~5−7 nm.

SEM

For all investigations, a scanning electron microscope (SEM) with field-emission gun was available (LEO Gemini 1530 VP, Zeiss, Germany). The orientation measurements were carried out using a commercial EBSD system (HKL Technology, Denmark) attached to the SEM. The diffraction patterns were collected under typical conditions: a light-sensitive digital camera captures the diffraction signal emitted from a sample tilted at 70º to the electron beam. The acceleration voltage of 15−20 kV was chosen to comply with the spatial resolution required. Because of the fast orientation interpretation, the EBSD technique is an ideal tool to analyse the orientation relationship between several phases in SEM. For post-analysis processing, the software package *Channel5* (also from HKL Technology) has been applied exclusively. A more detailed description of the EBSD

technique (also known as BKD − backscatter Kikuchi diffraction) as well as typical applications were given by Schwartz *et al*. (2000).

In conjunction with the EBSD investigations, chemical compositions were determined locally using energy dispersive spectroscopy (EDS). The system available was an INCA 2000 (Oxford Instr.) with a 'Premium'-Si(Li) detector and a Pentafet window (called ATW2).

Results

TEM characterization of carlsbergite in rhabdite

The lateral dimension of the majority of all observed rhabdite crystals in the foil produced was no bigger than 2 μm. These so-called microrhabdites (Clarke and Goldstein, 1978) were found to be free of precipitates. Carlsbergite was discovered only within rhabdites larger than ~5 μm (Fig. 2).

The EDS analysis of the CrN-inclusions adduced average values in the element concentrations of 48 at.% Cr and 49 at.% N (Table 1). The origin of the detected minor elements Fe and Ni is not clear, but Buchwald and Scott (1971) also reported the occurrence of these elements in CrN. This might indicate that they represent common substitutions in the carlsbergite structure. The crystallographic nature of the small precipitates has been confirmed unambiguously by selected area electron diffraction (SAED) experiments (Geist *et al*., 2005).

The TEM bright-field image in Fig. 1 shows a remarkable feature in the structures of the different phases. The surrounding kamacite is characterized by a high dislocation density. In contrast to that, the rhabdite crystals are dislocation-free; this becomes visible in the

TABLE 1. Chemical compositions of three different inclusions determined by TEM-EDS. The data for the inclusions A and B represent the average of five individual measurements.

| Inclusion | Element concentration (at.%) | | | |
	Cr	N	Fe	Ni
A	48(1)	48(2)	4(1)	0.2*
B	48(2)	51(2)	2(1)	0.1*
C	49(1)	49(2)	1(1)	0.2*

* This element occurs in concentrations that are close to the detection limit.

comparatively large bright areas and missing thin linear details. However, they do appear to be elastically strained. It is surprising, that the carlsbergite inclusions inside the rhabdite show a large number of dislocations. For the CrN inclusion, the dislocation density may be $>10^9$ cm^{-2}; for the kamacite it is even greater as it is virtually completely black, i.e. so full of dislocations that they appear as a dark mass.

Orientation relationships of carlsbergite and rhabdite determined by EBSD

Even the alignment of the few carlsbergite crystals in rhabdite, visible in the TEM foils, indicated that CrN is not randomly oriented in (Fe,Ni)$_3$P (Fig. 1). The EBSD investigations on 35 different carlsbergite individuals confirmed this observation. The majority of the brittle rhabdite rods are broken.

In Fig. 2, two carlsbergite precipitates within a rhabdite rod are visible. They are well aligned within the host crystal. In order to discover the orientation interaction, for each set of carlsbergite-rhabdite intergrowth one needs the orientation of the two crystals, determined by the interpretation of the respective EBSD patterns. The points where the EBSD patterns were collected are shown in Fig. 2. By a comparison of pole figures of low-indexed lattice planes, the orientation relationship between the two phases can be established (e.g. Nolze et al., 2004 , 2005). For example, in Fig. 3, the superimposition of a $\{100\}_R$ pole figure of rhabdite (black spots) and a surprisingly high-indexed $\{114\}_K$ pole figure of carlsbergite (grey spots) is represented.

Here a selected pole of each phase occupies the same position in the stereographic projection, which means that these phase-specific lattice planes are aligned parallel to each other giving at least one part of the orientation relationship. Unfortunately, the detected alignment of CrN in rhabdite is not uniform. Therefore we investigated all detectable carlsbergites which were visible in the studied piece of meteorite. Thirty five individual CrN crystals (discovered in 31 different rhabdites) gave six different orientation relationships. However, the orientation relationship of four individual CrN crystals could not be explained by the use of low indices. All of these are listed in Table 2 (see also Fig. 8).

Characterization of carlsbergite in kamacite

Although the north Chile iron is acknowledged as one of the weakly deformed meteorites, within the kamacite, numerous plain Neumann bands (shock-deformation twins in body centred cubic iron) are visible (also pointed out by Buchwald, 1975, pp. 930−931). In determining an orientation relationship, every orientation variation complicates the establishment of an intergrowth law. The orientation contrast in the back-scattered electron image (Fig. 4) indicates a locally deformed area around the plate CrN crystals. Moreover, the carlsbergites often exhibit fissures or they are broken. Also observed in the crumbled carlsbergite was some orientation change between
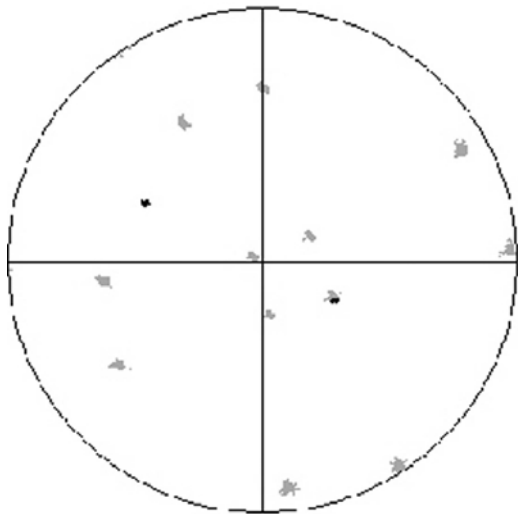

FIG. 3. The stereographic projection of superimposed pole figures: $\{100\}_R$ (black spots) and $\{114\}_C$ (grey spots). Note that rhabdite − having lower symmetry − yields only two poles in contrast to the cubic CrN.

FIG. 4. BSE image (orientation contrast) showing the fragmented platy CrN crystals in deformed kamacite.

the several parts and these produce a spread of data in the pole figures not only for kamacite but also for carlsbergite (Fig. 5). Therefore an unambiguous determination of the orientation relationship is difficult and should be a subject of further research.

Discussion

Carlsbergite detected in rhabdite rods

Almost all CrN crystals provided unambiguous orientation relationships. Similar to fcc/bcc phase boundaries, the interface between carlsbergite and rhabdite is characterized by close-packed lattice planes which appear parallel to each other. For rhabdite it is the $\{001\}_R$ which represents such a plane. In the unit cell of this mineral, the atoms are arranged in four layers aligned perpendicular to the c axis being located at ~0, ¼, ½ and ¾ of the unit-cell height. Each layer is composed of eight atoms with alternating metal and mixed metal-P layers (Fig. 6). The atoms belonging to one layer do not lie exactly at the same height but the deviations are negligible (<1.5%) for our purposes.

Because carlsbergite possesses the halite-type structure, the most closely packed atomic plane in this structure is $\{001\}_C$ followed by $\{110\}_C$. All observed orientation relations involve one or other of these layers. If the $\{110\}_C$ represents the plane of carlsbergite oriented parallel to $\{001\}_R$, the directions 100_R and 114_C in both lattices become parallel (see Table 2 and Figs 7, 8). In rare cases the measured angular deviations between the two directions are >2°.

When the $\{001\}_C$ plane of CrN is oriented parallel to the $\{001\}_R$ of the tetragonal rhabdite (Table 2), the mutual match of lattice vectors within the planes of these two phases is no longer unique. Instead, it appears that the rhabdite lattice vector 100_R matches more closely the vectors of carlsbergite. These represent a stepwise transition from 110_C to 140_C, which means a high orientation variation of ~30°. Figure 8 schematically demonstrates these orientation relation models. The numbers correspond to those given in Table 2.

FIG. 6. Crystal structures of rhabdite (*a*) and carlsbergite (*b*). The light-coloured spheres in rhabdite are the P atoms and the black spheres represent the metal atoms. The stacked atomic layers (which are equidistant from each other) marked by grey planes demonstrate the alternate layers occupied solely by metallic atoms (light and dark grey) and metal and phosphorus, respectively. The smaller darker grey spheres in the carlsbergite structure represent the N atoms.
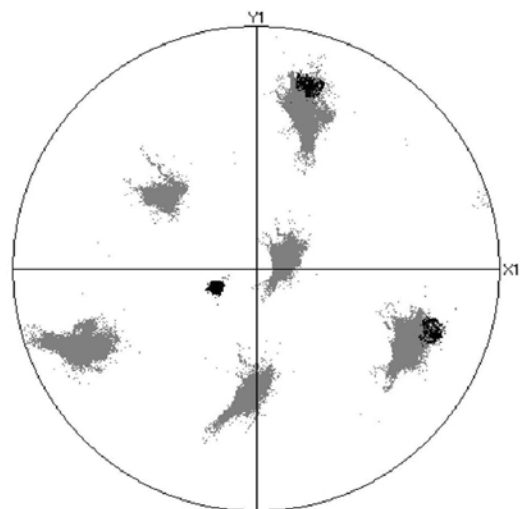
FIG. 5. Example of a pole figure: $\{001\}$ poles (black) of eight independent CrN crystals superimposed on the $\{110\}_k$ pole figure of the surrounding kamacite matrix (grey). Note the erratic shape and wide distribution of the kamacite poles, reflecting the deformation of the kamacite (cf. also Fig. 3).
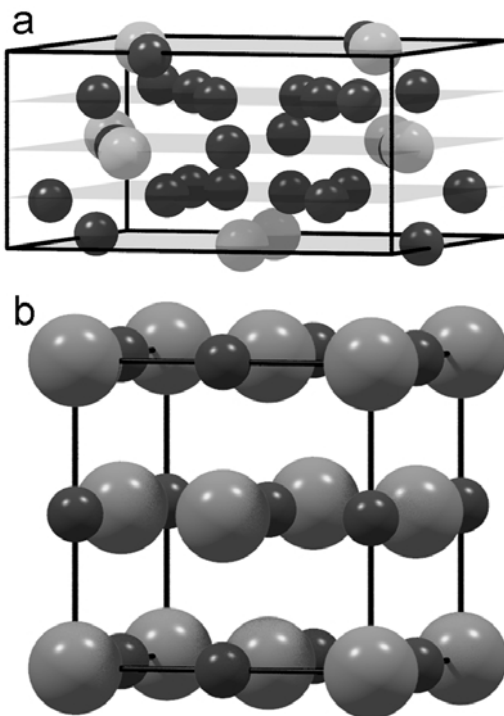
TABLE 2. Experimentally determined orientation relationships (OR) between 31 rhabdite precipitates and 35 individual carlsbergite crystals (2).

OR	Lattice planes	Lattice directions	Frequency	Misfit*
1	$\{001\}_R \parallel \{110\}_C$	$\langle 100 \rangle_R \parallel \langle 114 \rangle_C$	12	+2.8%
2	$\{001\}_R \parallel \{001\}_C$	$\langle 100 \rangle_R \parallel \langle 120 \rangle_C$	6	−2.5%
3	$\{001\}_R \parallel \{001\}_C$	$\langle 100 \rangle_R \parallel \langle 230 \rangle_C$	5	−1.7%
4	$\{001\}_R \parallel \{001\}_C$	$\langle 100 \rangle_R \parallel \langle 110 \rangle_C$	4	+2.8%
5	$\{001\}_R \parallel \{001\}_C$	$\langle 100 \rangle_R \parallel \langle 130 \rangle_C$	2	−1.5%
6	$\{001\}_R \parallel \{001\}_C$	$\langle 100 \rangle_R \parallel \langle 140 \rangle_C$	1	−0.1%
	no OR found		4	

* The misfit has been calculated using the lattice parameters a_C = 4.148 Å for carlsbergite and a_R = 9.040 Å for rhabdite (see text).

It is obvious that for each of the orientation relationships listed, a fair but not perfect lattice match exists (except for the four cases which did not show one of these simple interpretations). In all cases several CrN unit cells are necessary to demonstrate the lattice alignment graphically (Fig. 8). The large difference between the lattice parameters of rhabdite and carlsbergite are responsible for the multiple solutions. In order to compare the different solutions found quantitatively, the lattice mismatch was calculated:

$$\frac{\Delta d}{d} = \frac{d_C - d_R}{d_R} \ .$$

This misfit describes the deviation of both lattices for the given orientation relation, i.e. for case 4 in Fig. 8 it compares the length of three steps in the $\langle 100 \rangle_C$ direction (d_C) with that of one step in the $\langle 110 \rangle_R$ direction (d_R). The misfit calculated varies between −2.5% and +2.8% (Table 2). The distribution of lattice misfit data shows that no simple correlation exists between the number of detected orientation relations and the value of the misfit. However, it should be noted that these calculations have been performed by use of the selected lattice parameters a_C = 4.148 Å and a_R = 9.040 Å. The value for rhabdite was calculated using the measured Fe:Ni ratio of ~1.34 (Fig. 1) and the experimentally determined dependence of the lattice parameter on the Fe/Ni ratio of the phosphides (Skála and Drábek, 2000). For other values which are possible for schreibersite (see also Skála and Císařová, 2005) or other ambient conditions (elevated temperatures), the magnitude of the misfit would differ.

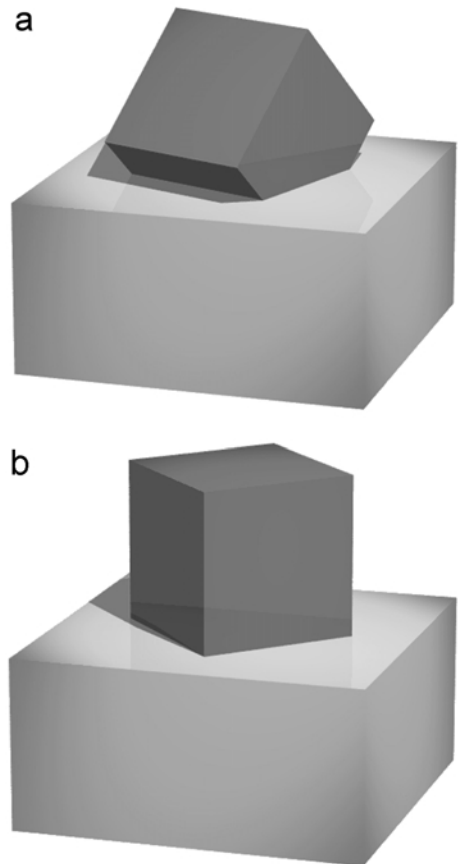Following the comparison of the unit-cell dimensions, details of the atomic structure can

FIG. 7. Illustration of the main orientation relations between rhabdite and carlsbergite from Table 2: (*a*) shows case no. 1, i.e. $\{001\}_R \parallel \{110\}_C$, and (*b*) displays $\{001\}_R \parallel \{001\}_C$ for case no 4.
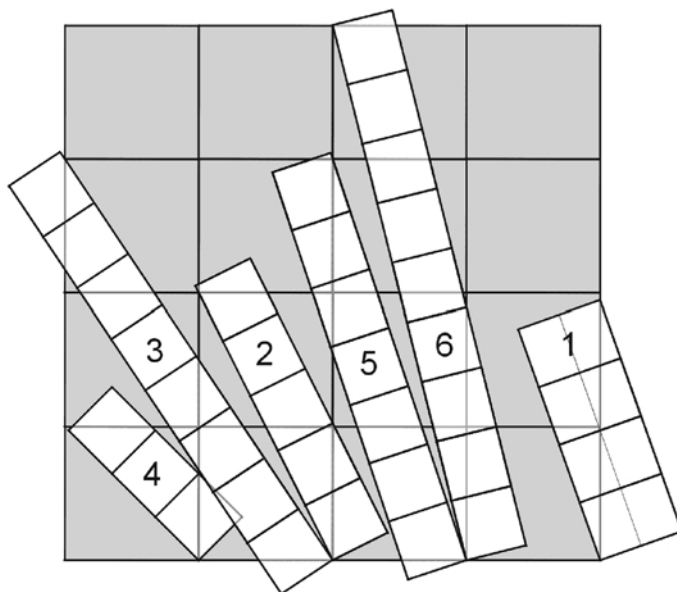
FIG. 8. Projections of carlsbergite unit cells (white squares) onto a $\{001\}_R$ (grey squares). The numbers correspond to the different orientation relationships (OR) listed in Table 2. Note, that the OR1 is not based on the cubic plane of CrN but on the rectangular plane $\{110\}_C$.

now be considered. In Fig. 9, the most frequent orientation relation (No. 1) is shown. There, a mixed-metal-P layer of rhabdite is illustrated. Figure 9a shows a row of four carlsbergite unit cells oriented with $\{110\}$ parallel to the plane of the paper with the $\langle 114 \rangle_C$ placed parallel to $\langle 100 \rangle_R$. Obviously, either P or metal atoms may coincide with the contour of the CrN cells. The start and end points of the $\langle 114 \rangle_C$ vector overlap equivalent P atoms in the rhabdite structure. The directional distribution of atoms within the rhabdite layer $\{001\}_R$ reveals only a few distinct directions which correspond to the detected orientation relation. In Fig. 9b, lines parallel to $\langle 001 \rangle_C$ have been inserted to be consistent with the assumption of $\langle 114 \rangle_C \parallel \langle 100 \rangle_R$. It is remarkable that all atoms fit this network of lines. In this particular case the match of atomic positions exists only for the metal- P layer.

For all other detected orientation relations (Table 2), we also found a good correlation between the atomic arrangements in rhabdite and carlsbergite structures.

Dislocations

As mentioned above, the sample investigated is characterized by a high dislocation density which can be ascribed either to the effect of the plastic deformation (cold working) and/or to lattice mismatch. Moreover, the different thermal expansion of the materials and particularly the anisotropic expansion behaviour of the tetragonal schreibersite (Nye, 2000) could also be an additional source of dislocations. However, the rhabdite shows virtually no dislocations but only a strong elastic deformation. Due to the different mechanical behaviour of the ductile kamacite and the brittle rhabdite, the deformation mode differs. While the metal deforms plastically (cf. the varying orientation contrast within kamacite shown in Figs 2 and 4), which results in a high dislocation density (e.g. Leroux, 2001), the phosphides appear to be, at most, elastically strained (no orientation contrast in Fig. 2, but also no visible dislocations in Fig. 1). If the strain is too high the phosphides show brittle fracture: the rods fracture in several pieces perpendicular to their axes (Fig. 2). The most surprising result concerns the dislocation structure in carlsbergite, surrounded by a rhabdite crystal which is dislocation-free.

The hardnesses of CrN and $(Fe,Ni)_3P$ are comparable (Hölzel, 1989) and both materials are brittle. Hence, the different symmetries of both crystals ($I\bar{4}$ and $Fm\bar{3}m$) might be responsible
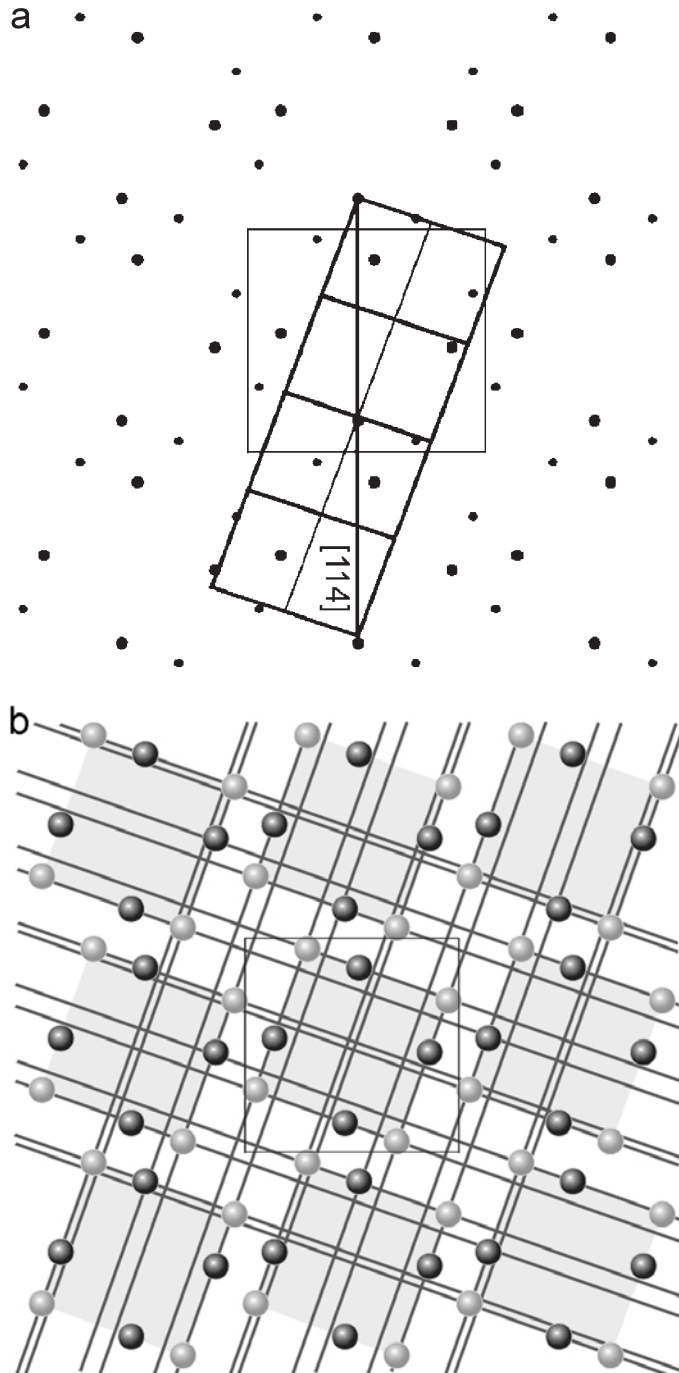
a

[114]

b

FIG. 9. Atomic match of carlsbergite (four unit cells) and a metal-P-layer of rhabdite for the most frequently detected orientation relation: $\{001\}_R \parallel \{110\}_C$ and $\langle 100 \rangle_R \parallel \langle 114 \rangle_C$ (No. 1) (*a*). The atoms of the rhabdite structure are well aligned along special directions correlating with the detected orientation relation (*b*). The inserted grey squares underline the alignment of atoms parallel to the superimposed lines.

for this behaviour, i.e. due to the distinct lower symmetry of the schreibersite, the nucleation and propagation of dislocations are complicated. In order to check this assumption, xenomorph schreibersite, ideomorph rhabdite and thin schreibersite lamellae of a related iron meteorite (Sikhote − Alin) have been studied by TEM. Even for this additional sample no dislocations were found within schreibersite/rhabdite crystals, in contrast to the surrounding kamacite which is always highly dislocated. This means, independent of the Fe/Ni-ratio (1.43−4.41) and the different formation temperatures (Clarke and Goldstein, 1978) of the phosphides, every type is dislocation-free. Therefore, the different crystal structures of both seem to influence the formation of dislocations. Detailed investigations are necessary in order to clarify this phenomenon.

If the rhabdite does not show dislocations, why does the embedded CrN need to form dislocations? Assuming that the precipitation of CrN predates that of rhabdite (Buchwald, 1975, p. 923, Randich and Goldstein, 1978) carlsbergite grains can act as nuclei for the formation of the larger rhabdite crystals. In this case the carlsbergites could contain large numbers of dislocations because they were once a part of the deformed matrix. If the CrN crystals are primarily formed in the metallic matrix then their orientation relationship to the metal should be the original one. Later, some of the rhabdites formed enveloped the carlsbergites and some secondary relationships between CrN and rhabdite (2) were produced because of their different structures. These relations are described in this paper. Since a distinct orientation relationship beween the rhabdites and kamacite exists, a connection of all these relations should exist. Unfortunately, the deformations, characteristic of the iron meteorites, complicate the determination of the orientation relation, e.g. between CrN and kamacite. A forthcoming paper examines these problems.

Summary and conclusions

The crystallographic features of the minor phases schreibersite (i.e rhabdite) and carlsbergite appearing in the north Chile iron meteorite were studied. The orientation relations were determined using the EBSD technique and can be interpreted based on the lattice dimensions as well as the atomic configuration of the phases involved. It was found that the minute carlsbergite (CrN) crystals are not only located at the surface of the idiomorphic rhabdites but also within them. The intergrowth of kamacite and CrN, which are both cubic, probably produces a single orientation relationship whereas rhabdite (tetragonal) and carlsbergite (cubic) have several specific orientation relations. In all cases a certain misfit along the phase boundaries was detected. The high dislocation density can be ascribed to this lattice mismatch or/and to the effect of the plastic deformation (cold working). The absence of dislocations in rhabdite, in contrast to carlsbergite and kamacite, is surprising and needs further investigation. If we assume that the formation of CrN predates that of rhabdite then the orientation relation between carlsbergite and rhabdite is of secondary character and the basic orientation relation is that between CrN and the metallic matrix. Other iron meteorites should be studied to confirm whether the orientation relations and other phenomena observed in the north Chile iron meteorite occur elsewhere.

References

Axon, H.J., Kinder, J., Haworth, C.W. and Horsfield, J.W. (1981) Carlsbergite, CrN, in troilite, FeS, of the Sikhote Alin meteoritic iron. *Mineralogical Magazine*, **44**, 107−109.

Bøggild, O.B. (1927) The meteoritic iron from Savik near Cape York. *Meddelelser om Grønland*, **74**, 11−30.

Buchwald, V.F. (1975) *Handbook of Iron Meteorites*. University of California Press, USA, 1375 pp.

Buchwald, V.F. and Scott, E.R.D. (1971) First nitride (CrN) in iron meteorites. *Nature Physical Science*, **233**,113 −114.

Clarke, R.S. and Goldstein, J.I. (1978) Schreibersite growth and its influence on the metallography of coarse-structured iron meteorites. *Smithsonian Contribution to Earth Science*,. Report no **21**, Smithsonian Institution.

Doenitz, F.D. (1970) Die Kristallstruktur des meteoritischen Rhabdites $(Fe,Ni)_3P$. *Zeitschrift für Kristallographie*, **131**, 222−236.

Fultz, B. and Howe, J.M. (2005) *Transmission Electron Microscopy and Diffractometry of Materials.* Springer Berlin, 748 pp.

Geist, V., Wagner, G., Nolze, G. and Moretzki, O. (2005) Investigation of the meteoritic mineral $(Fe,Ni)_3P$. *Crystal Research and Technology*, **40**, 52−64.

Grady, M.M., editor (2000) *Catalogue of Meteorites.* Cambridge University Press, Cambridge, UK, 689 pp.

He, Y., Godet St., P.J.J and Jonas, J.J.(2006) Crystallographic relations between face- and body-centred cubic crystals formed under near-equilibrium conditions: Observations from the Gibeon meteorite. *Acta Materialia*, **54**, 1323−1334.

Headley, T.J. and Brooks, J.A. (2002) A new bcc-fcc orientation relationship observed between ferrite and austenite in solidification structures of steels. *Metallurgical and Materials Transactions*, **A**33, 5−15.

Hennig, C., Geist, V. and Heide, G. (1999) Investigation of the rhabdite/kamacite law of intergrowth in iron meteorites with the aid of the Kossel effect. *Meteoritics and Planetary Science*, **34**, 61−66.

Hölzel, A.R. (1989) *Systematics of Minerals.* Published by the author, Mainz, Germany, 584 pp.

Leroux, H. (2001) Microstructural shock signatures of major minerals in meteorites. *European Journal of Mineralogy*, **13**, 253−272.

Moretzki, O., Morgenroth, W., Skála, R., Szymanski, A., Wendschuh, M. and Geist, V. (2005) Determination of the metal ordering in meteoritic $(Fe,Ni)_3$ P crystals. *Journal of Synchrotron Radiation*, **12**, 234−240.

Nasreddine, M., Bertaut, E.F., Roubin, M. and Paris, J. (1977) Crystallographic study of low-temperature $Cr_xV_{1-x}N$. *Acta Crystallographica*, **B33**, 3010−3013.

Nolze, G. and Geist, V. (2004) A new method for the investigation of orientation relationships in meteoritic plessite. *Crystal Research and Technology*, **39**, 343−352.

Nolze, G., Geist, V., Saliwan Neumann, R. and Buchheim, M. (2005) Investigation of orientation relationships by EBSD and EDS on the example of the Watson iron meteorite. *Crystal Research and Technology*, **40**, 791−804.

Nye, J.F. (2000) *Physical Properties of Crystals.* Clarendon Press, Oxford, UK, 329 pp.

Randich, E. and Goldstein, J.I. (1978) Cooling rates of seven hexahedrides. *Geochimica et Cosmochimica Acta*, **42**, 221−233.

Schwartz, A.J., Kumar, M. and Adams, B.L. (2000) *Electron Backscatter Diffraction in Material Science.* Springer, The Netherlands, 350 pp.

Schwarzer, R.A. and Sukkau, J. (2003) Automated evaluation of Kikuchi patterns by means of Radon and fast Fourier transformation, and verification by an artificial neural network. *Advanced Engineering Materials*, **5**, 601−606.

Sevillano, J.G., García-Rosales, C., Echeberria, J.J. and Zubillaga, Y.C. (2000) Structure and crystallographic texture of a metallic meteorite of octahedrite type (Gibeon). *Boletin Sociedad Española de Ceramica y Vidrio*, **39**, 313−318.

Skála, R. and Císařová, I. (2005) Crystal structure of meteoritic schreibersites: Determination of absolute structure. *Physics and Chemistry of Minerals*, **31**, 721−732.

Skála, R. and Drábek, M. (2000) *Variation of unit-cell dimensions of experimentally synthesized members of Fe_3P-Ni_3P solid solution* (abstract # 1564). 31st Lunar and Planetary Science Conference, CD-ROM.

Zipfel, J., Kim, Y. and Marti, K. (1995) Nitrogen isotopic disequilibrium in the Cape York IIIA iron. *Meteoritics*, **30**, 606.

Zucolotto, M.E. and Pinto, A.L. (2000) Electron back-scattered diffraction studies of the Barbacena meteorite. *Meteoritics and Planetary Science*, **35**, supplement, p. A180 (abstract).

Zucolotto, M.E. and Pinto, A.L. (2001) A metallographic and EBSD study of the Maria Da Fé iron. *Meteoritics and Planetary Science*, 36, supplement, p. A234 (abstract).